Online Structural Health Monitoring of Wire Rope by Fiber Optic Low Coherence Interferometric Sensor

Z. DJINOVIC, M. STOJKOVIC and M. TOMIC

ABSTRACT

In this paper we use an intrinsic fiber-optic sensor for detection of acoustic-emission (AE) events occurring in the metal rope. Basic principle of operation is low-coherence interferometry performed as an “all-in-fiber” Michelson interferometer. The core part of the sensing setup is 3x3 coupler made of single-mode optical fiber operating at 1300nm of light wavelength. The coupler provides a passive stabilization of the interferometric signal by generation of two quadrature signals. The sensing element is made of fiber-optic coil of 25mm in diameter, wrapped around the Al disk that is bonded to the rope. We tested a metal rope of 5mm in diameter and length of 1000mm. The rope has been loaded in a metal frame till to about 4000kN.

INTRODUCTION

Structural health monitoring of wire rope in service is very important task having in mind rather broad field of application of this constructive element. Basically, an *on line* wire rope monitoring technique has to fulfill a couple of requirements [1, 2]: light weight and easy operation, examination under service without major interruption, etc. Currently, in wide use of testing of metal ropes is magnetic technique. However, the method, being relies on movement, can’t work *on line.* The acoustic-emission (AE) method of inspection has the potential to satisfy the above requirements. The phenomenon behind an AE is generation of transient elastic waves by rapid release of energy. Within a wire rope in service the main sources of detectable AE include wire break, inter-wire fretting, corrosion and emission at termination of the rope into the steel socket. When the AE reaches the surface of the subjected material, the small displacements they produce are usually detected by piezoelectric transducers.

Zoran Djinovic, Integrated Microsystems Austria, Viktor Kaplan str. 2, 2700 Wr. Neustadt, Austria
Marijana Stojkovic, Integrated Microsystems Austria, Viktor Kaplan str. 2, 2700 Wr. Neustadt, Austria
Milos Tomic, School of Electrical Engineering, University of Belgrade, Bul. Kralja Aleksandra 73, 11120 Belgrade, Serbia

The first known study into the application of acoustic-emission technology to wire rope applications was carried out by Laura [3, 4]. The author used accelerometers clamped to 10 mm diameter rope, of various construction and length, to detect wire breaks at about 95% of the maximum load during raising the load-test to failure. Their work showed that wire breaks detected before failure of the rope were 15-20 dB above background noise.

Extensive research of application of AE technique for evaluation of the wire ropes was carried out at University College, Cardiff during the period 1980-1987. Most of the work was conducted using 11 and 12 mm diameter six-strand rope, with limited amount of work conducted on 40 mm six-strand rope. Taylor and Casey [5] showed that was possible to detect and discriminate wire breakage from background noise sources. Further, Casey and Taylor [6], and later Holfolrd [7], demonstrated that event of wire breakage can be located with reasonable accuracy. They also showed that wire breakage can be detected in 12 mm rope over distance of about 30 m. Holford [7] was successful in detecting outer-wire breaks up to distance of 46 m using various six-strand ranging in diameter from 10 to 28 mm and piezo-electric transducers. The energy of the signal resulting from a wire break is proportional to wire diameter. The implication of this is that the mechanical energy produced during the fracture process is proportional to the acoustic energy released and the strain energy. It is proposed that the proportions by which these forms of energy are divided are governed by Young's modulus. Rebel et al. [8] gave a detailed analysis of various condition monitoring techniques for fiber mooring ropes used in offshore applications where magnetic techniques cannot be applied. Different approaches to condition monitoring were listed.

In this paper we use an intrinsic fiber-optic sensor for detection of AE events. The sensor was firmly fixed to the subjected metal rope. Basic principle of operation is low-coherence interferometry performed as an "all-in-fiber" Michelson interferometer. The core part of the sensing setup is 3x3 coupler made of single-mode fiber operating at 1300 nm of light wavelength. The coupler provides a passive stabilization of the interferometric signal by generation of two quadrature signals. The sensing element is made of fiber-optic coil of 25 mm in diameter, wrapped around the Al disk that is bonded to the rope. We tested a metal rope of 5mm in diameter and length of 1000 mm. The rope has been loaded in a metal frame till to about 4000 kN. We accomplished parallel measurements of AE of the rope by commercial system of Physical Acoustics Corporation [9]. A brake of the wire has been simulated by so called "pencil test". After signal processing, we obtained demodulated signals expressed as a phase change in dependence on the acquisition time. The signals contained a broad range of frequency components so we made a high pass filtration with cut off at 3 kHz. In this way we obtained a pure acoustic signal with several characteristic patterns showing an abrupt change in the optical phase of the sensing interferometer. Rise time was in the order of 0,5-1 µs. Signal modulation was about ±1,5 rad that was far away from the signal noise of about ±0,05 rad. It corresponds to SNR of about 30 dB. We can also estimate the duration time of the AE signal of about 18 ms that corresponds with literature results.

PRINCIPLE OF OPERATION

The sensing configuration is basically an “all in fiber” Michelson interferometer, where splitting and combining of beams are done by a 3x3 single-mode fiber optic coupler, Fig. 1.

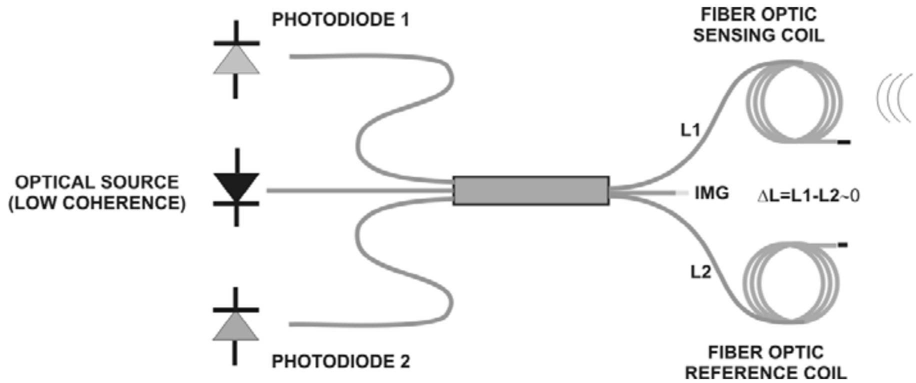

Figure 1. Schematic presentation of an “all-in-fiber” Michelson interferometric sensing configuration based on 3x3 single-mode fiber optic coupler.

The use of the 3x3 single-mode coupler brings us two quasi-quadrature interferometric signals, mutually shifted by $2\pi/3$ rad, which can be combined in a special way to obtain a stable interferometric signal [10-12]. The low coherence interferometry is employed in order to avoid some problems characteristic for high coherence interferometric measurement systems: parasitic interferences and instabilities of the optical source frequency/phase caused by back-reflections. The principle of operation and some details of proposed configuration, shown in Fig. 1, are given below. Low coherence optical source (superluminescent diode at 1300nm) is coupled into the middle input arm of the 3×3 fiber coupler, two receiving photodiodes are connected to the two other input arms. The sensing coil (about 25mm in diameter, made of 5 turns of single-mode fiber 9/125/250 µm) is attached to one of output arms. A fiber optic coil of the same size and turns like previous, called referencing coil, is attached to the second coupler output arm. The middle output arm is immersed into the index matching gel (IMG), in order to avoid the back reflection from this unused fiber end. The beam back-reflected from the fiber ends have been recombined inside of the 3×3 coupler. In this way, two quasi-quadrature interferometric signals, are produced and subsequently captured by two photodiodes.

The photodiode signals have, in ideal case, following shapes [11]:

$$\begin{aligned} i_{PD1} &= I_0\left\{1+V\exp\left[-\left(2\Delta L/L_C\right)^2\right]\cos\left(\frac{2\pi}{\lambda}\left(\Delta L+\Psi(t)\right)\right)\right\} \\ i_{PD2} &= I_0\left\{1+V\exp\left[-\left(2\Delta L/L_C\right)^2\right]\cos\left(\frac{2\pi}{\lambda}\left(\Delta L+\Psi(t)\right)+\frac{2\pi}{3}\right)\right\} \end{aligned} \tag{1}$$

where I_0 is the maximum photodiode current, V is the fringe visibility, ΔL is the “static” optical path difference between the sensing and reference coils, L_C is optical source coherence length, λ is the optical source wavelength and $\Psi(t)$ is phase disturbance caused by impinging acoustic waves.

An external force that acts on the fiber coil carrying optical radiation, induces the phase change, i.e. change of the optical path length in the sensing arm. The induced phase change can be expressed by:

$$d\Psi = k \cdot d(n \cdot L) = k \cdot L \cdot \left(n\frac{dL}{L} + dn \right) \tag{2}$$

where k=2π/λ, n is the refractive index of glass in the core region and L is the overall sensing length of the fiber. L is equal to 2πRN, where R is the coil radius and N is the number of the turns. The term ndL reflects the physical change of the fiber length while the term Ldn reflects the change of the refraction index of the glass. The phase response on the strain approximately has a linear form:

$$d\Psi = k \cdot \gamma \cdot n \cdot dL \tag{3}$$

where γ is optical strain correction factor that for silica glass fiber is ~0.78. In that way, the intensity of impinging acoustic wave can be determined from the measured phase change.

EXPERIMENT

In Fig. 2 we schematically present experimental set up for characterization of interferometric principle of fiber-optic sensor. We tested metal rope of about 5mm in diameter and length of 1000mm. The rope has been loaded in metal frame till to about 4000kN (Fig. 2 and 3). We accomplished parallel measurements of acoustic emission of the rope by commercial system of Physical Acoustics Corporation [9]. For this purpose we equipped the rope with three PZT sensors bonded by epoxy glue at distance of 0, 500 and 1000 mm of the rope according the schedule shown in Fig. 2. Fiber-optic sensor was bonded in a close proximity to the PZT 3.

A brake of the wire has been simulated by so called “pencil test”. The pencil break tests were conducted to ensure the sensitivity of each PZT and FOS sensor. In Fig. 2 we depicted those points along the rope that were exposed to the pencil break test. The separations are 125, 250, 750 and 875 mm starting from PZT 3. We repeated the test five times per every point in order to investigate reproducibility of both sensor types.

Generally, the set up consists of fiber-optic and optoelectronic part. Central fiber-optic part is 3x3 fused coupler with three input and three output arms made of single mode optical fiber of 9/125/250 µm in diameter, optimized for transmission light wavelength of about 1330 nm. One input arm is connected to the light source, a superluminescent diode (SLD) emitting at 1310 nm. Light comes in the coupler and further splits in the three arms: sensing, reference and inert arm. The fiber end of the last arm is immersed into index matching gel in order to suppress the parasitic back reflection.

The sensing arm is in the form of coil composed of 5 turns around Al disk of 25 mm in diameter and 3 mm in width (Fig. 3). The disk is firmly fixed to the rope using epoxy based 2K structural adhesive. The reference arm also has a form of coil wrapped in the same way as sensing coil. The end of the reference arm was settled against mirror, firmly fixed on movable scanning stage. By this stage we adjusted the interferometer in balance ready for measurement. This coil, as well as 3x3 coupler has been enclosed in a metal box. When optical phase difference between the sensing and reference coil is in the range of optical coherence of SLD (of about 30 µm) we obtain interference. It always appears when an external stimulus, such as acoustic wave emitted after the wire break, disturb the balance of interferometer by causing alternation of optical path length in the sensing coil. The interferometric effect has been detected by two InGaAs photodiodes in optoelectronic unit and further acquired with NI A/D card, typically with acquisition rate of 600 Msample/s/channel in duration of 1,5s.

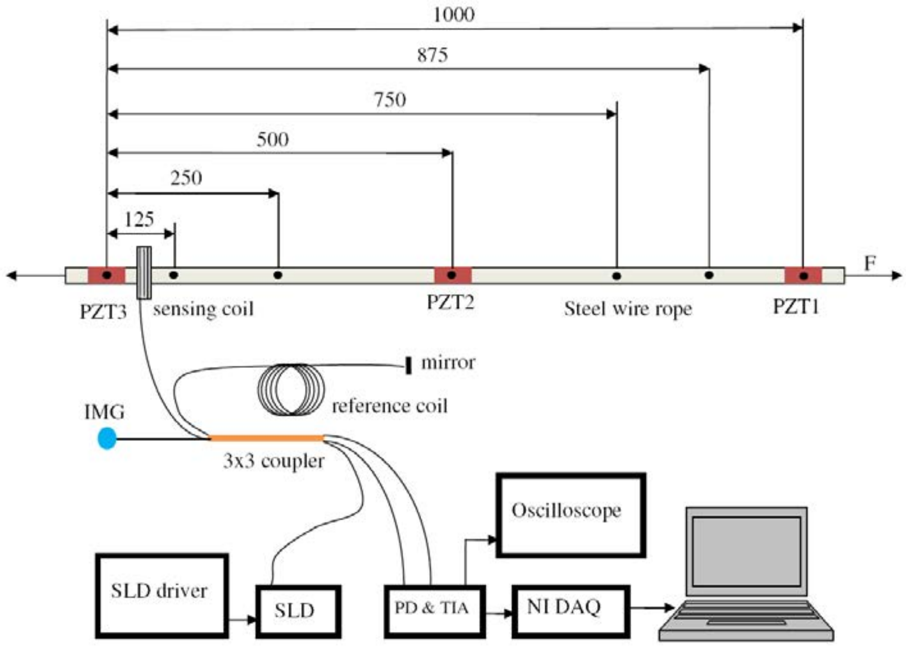

Figure 2. Basic sensing configuration for experimental test of interferometric principle of fiber-optic sensor; SLD-superluminescent diode, PD&TIA-photodiodes and transimpendance amplificator, NIDAQ-National Instrument Digital/Analog card of 16 bit and sampling rate of 1,2 Msample/s, PZT-piezoceramic actuator/sensor, IMG-index matching gel.

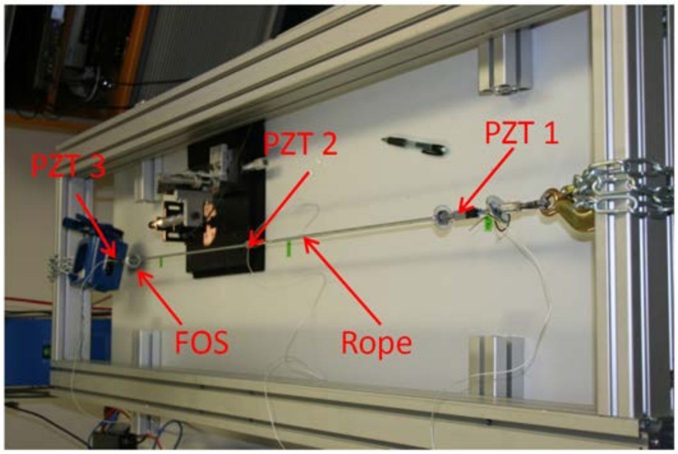

Figure 3. Metal rope under test equipped with three PZT sensors and one fiber-optic sensor: Length 1000mm, diameter 5mm, load app. 4000kN.

RESULTS AND DISCUSSION

We will now present results of investigation of fiber-optic sensor after simulation of wire break by pencil test. We obtained very similar results for all aforementioned (Fig. 2) separations between the excitation points and fiber-optic sensor. Therefore, we choose just one separation of 250 mm to go through the explanation of breaking phenomena and generation and acquisition of AE event.

In Fig. 4 we present already processed two raw interferometric signals using “arctan” algorithm implemented in MatLab software. This diagram presents demodulated interferometric signal expressed as a phase change given in (radian) in dependence on time given in (ms). We can clearly see the moment of breaking event at about 730 ms. It appears as an AC signal having rather large modulation of about ±15 rad in maximum and lasting time more than 800 ms. Probably it was larger but in this case we were limited with duration of the acquisition time of 1,5 s.

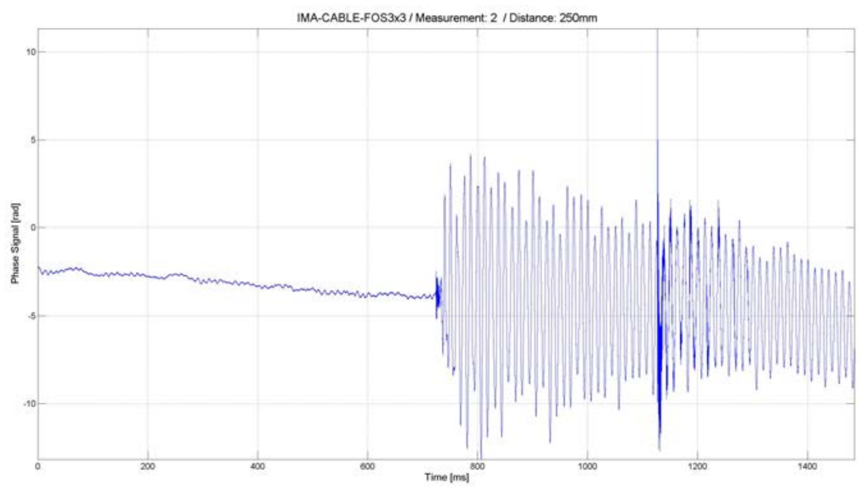

Figure 4. Demodulated raw interferometric signals acquired by two photodiodes for separation of fiber-optic sensor from wire excitation by pencil test of 250mm, an AE event occurred by the break of the pencil core simulating the brake of the wire in the metal rope of 5mm in diameter and 1000mm length.

However, above signal does not present the acoustic emission (AE) signal immediately. It contains a wide frequency range, so in order to extract the useful AE signal only, we have to make filtration using high pass filter (cut off at 300kHz). Fig. 5 shows the signal after filtration when low frequency components are omitted. In this way we obtained a pure acoustic signal with several characteristic patterns. The first one started at about 730 ms and presents the real acoustical response of the fiber-optic sensor after the pencil break test. The second pattern, or more precisely a train of seven patterns, is probably the back reflected acoustic signal from the end of the rope. Perhaps, the back reflected signals interfered with the initial AE signal and as a result they have got larger amplitudes than the original signal.

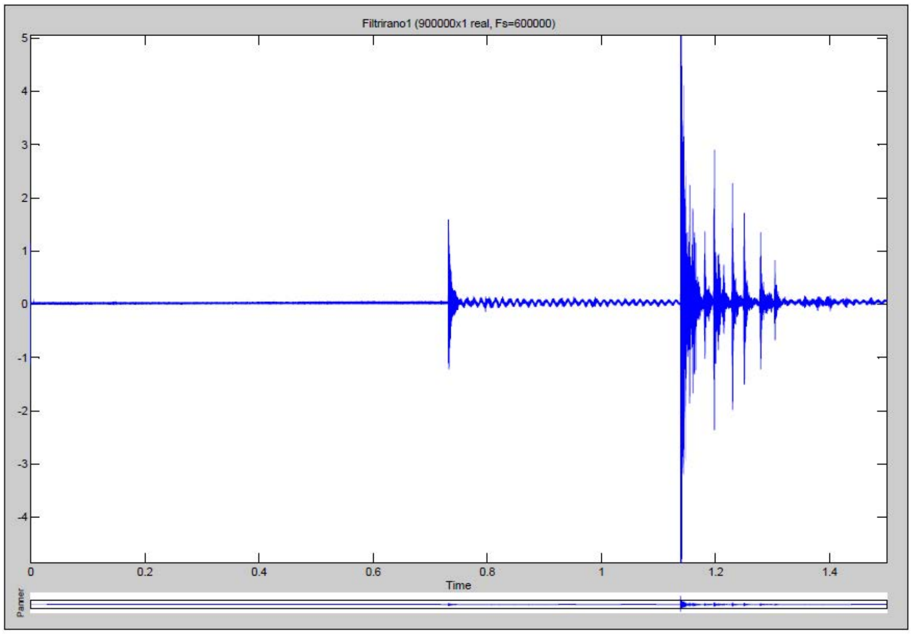

Figure 5. Signal processing by high pass filtration of the demodulated signal denoting a full record of the acoustic emission events occurred by the break of the pencil core simulating the brake of the wire in the metal rope of 5mm in diameter and 1000mm length, Y axis: Phase signal (rad), X axis: Time (s).

In Fig. 6 we present a detail from the above picture in order to show the structure and duration of the initial AE signal recorded immediately after the breaking event. We can see now an abrupt change in the optical phase of the sensing interferometer. Rise time is in the order of 0,5-1 μs. Signal modulation is about ±1,5 rad that is far away from the signal noise that is of about ±0,05 rad. It corresponds to SNR of about 30 dB. We can also estimate the duration time of the AE signal and it is about 18 ms that corresponds with results of other researchers [13].

Further, we performed FFT analyze on the complete demodulated signal given in Fig. 4 and on the filtered signal given in Fig. 5. Fig. 7 presents the power spectrum of the complete signal having two characteristic frequency peaks in the low frequency range at 79 and 111 Hz. These peaks occur as a consequence of mechanical vibrations after touching the wire rope with pencil core during the execution of the pencil break test.

In Fig. 8 we present power spectrum of filtered signal with characteristic peaks in the high frequency range at about 3370 and 6300 Hz. These peaks appear as a result of pure acoustic emission of pencil brake and they are in good agreement with findings of other groups [13].

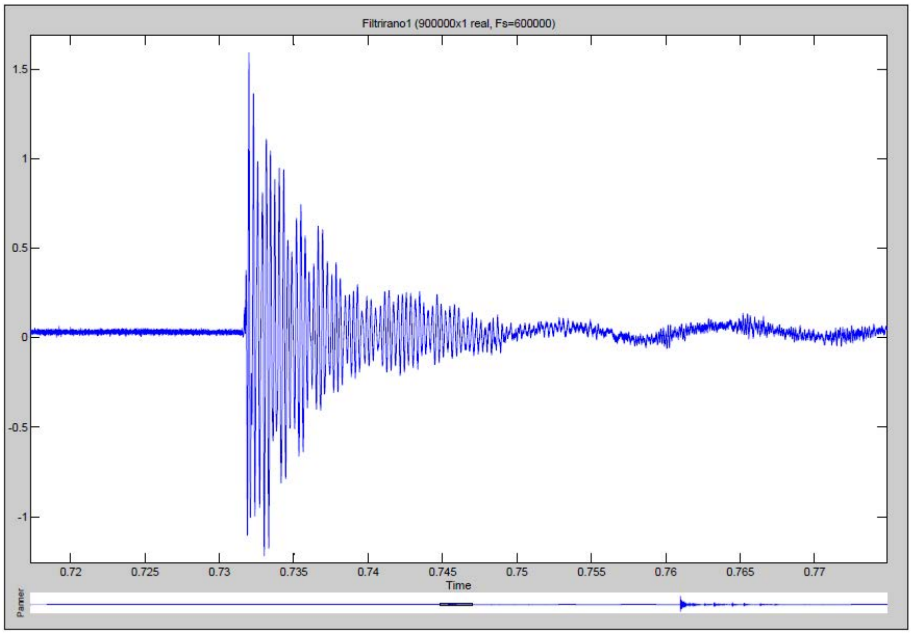

Figure 6. Close look at the signal in Figure 5 denoting a record of acoustic emission events occurred by the break of the pencil core simulating the brake of the wire in the metal rope of 5mm in diameter and 1000mm length, Y axis: Phase signal (rad), X axis: Time (s).

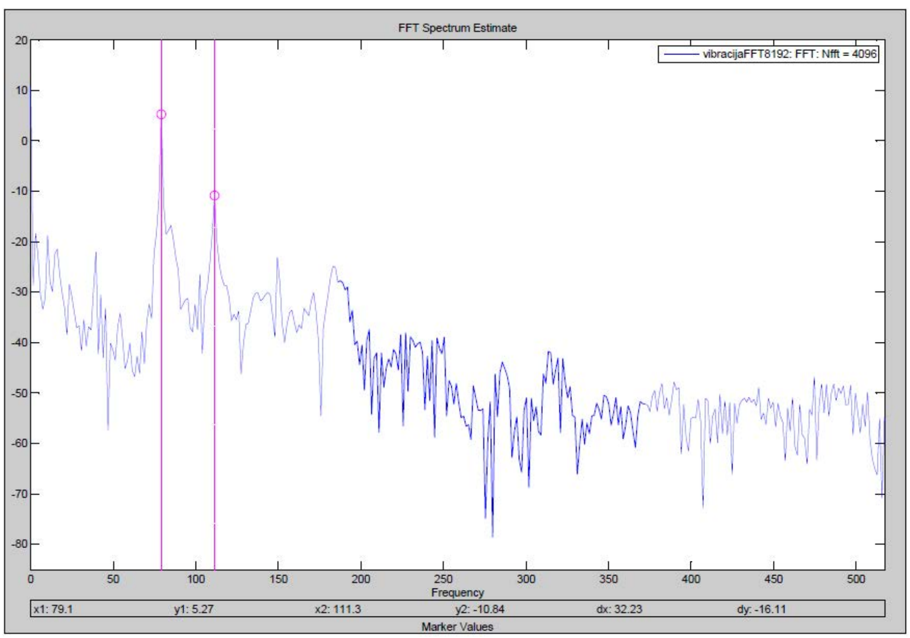

Figure 7. Signal power spectrum after FFT analyze denoting two characteristic peaks in the low-frequency range (79 Hz and 111Hz), acoustic emission events in the low-frequency range occurred by mechanical vibrations of the rope during the pencil test simulating the brake of the wire in the metal rope of 5 mm in diameter and 1000 mm length, Y axis: Power spectrum (dB), X axis: Frequency (Hz).

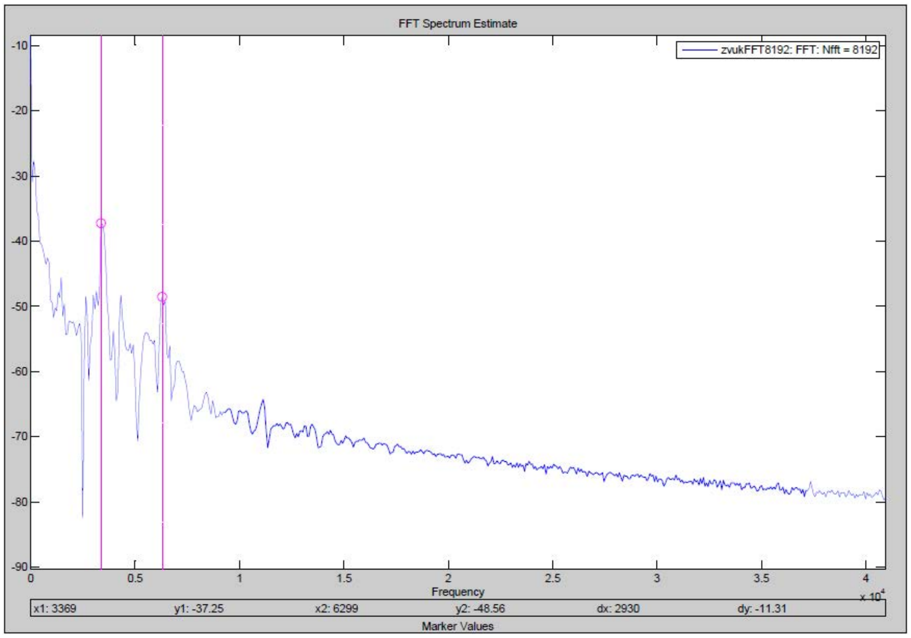

Figure 8. Signal power spectrum after FFT analyze denoting two characteristic peaks in the high-frequency range (3369 Hz and 6299 Hz), acoustic emission events in the low-frequency range occurred by mechanical vibrations of the rope during the pencil test simulating the brake of the wire in the metal rope of 5 mm in diameter and 1000 mm length, Y axis: Power spectrum (dB), X axis: Frequency (Hz).

In Table 1 we summarized the average values of maximal amplitude of optical phase modulation for all four separations between the fiber-optic sensor and excitation point by the pencil break test.

Table 1: Dependence of amplitude of phase modulation on separation of AE event.

Separation (mm)	Phase signal (rad): peak-peak
125	1,40
250	1,90
750	1,27
875	0,57

Data in Table 1 show that amplitude of phase modulation basically decreases with increase of separation of AE event from fiber-optic sensor. However, it is quite difficult to make any serious conclusion about attenuation of acoustic emission signal in our experiment. At first, because we had not regular conditions for the pencil break test. It means that coupling efficacy between the pencil and rope was not always the same and because of that the acoustic energy has not been equally transported. Second, the rope length of 1000 mm was too short to be able to collect the reliable data that we could use for evaluation of attenuation of acoustic emission waves.

However, literature results [13], show that acoustic emission events can be detected till to 46 m for the rope of 10 to 28 mm using piezo-transducers. Parallel measurements that we performed in this investigation using commercial Physical Acoustics System show that SNR for the tested rope was in the range of 56 and 90 dB depending on the separation between the point of the pencil test and PZT sensor.

Fiber-optic interferometric sensors are known as very sensitive devices that can detect phase shift in the ineterferometer till to picometer range [14]. Therefore, we expect to reach the same or even better sensitivity after optimization of the whole sensing system.

CONCLUSION

We tested and experimentally proved low-coherence interferometric technique performed as “all-in-fiber” sensing configuration for passive detection of the acoustic emission events. The AE events have been generated by pencil break test that simulated the single wire break in the metal rope of 5 mm in diameter and 1000 mm in length. Sensing configurations is based on the fiber-optic coil firmly bonded to the subjected rope. We found that lasting time of the AE signals is about 20 ms in the high-frequency range at about 3370 and 6300 Hz that is in good agreement with results of other authors.

REFERENCES

1. R. A. Egan, “Non-destructive testing of wire ropes”, Ninth Annual Offshore Technology Conference, Houston, TX, OTC 2926, pp. 375-381 (1977)
2. H. Babel,”Destructive and non-destructive methods to determine the life of wire ropes”, *Wire* 28 (1979) 263-270
3. P. A. A. Laura, “Acoustic detection of structural failure of mechanical cables”, Journal of the AcousticsSociety of America 45 (1969)791
4. P. A. A. Laura, “Mechanical behaviour of stranded wire rope and feasibility of detection of cable failure”, Marine Technology Society Journal 4 (1970)19
5. J. L. Taylor, N. F. Casey, “The acoustic emission of steel wire ropes”, Wire Industry 5 (1984)79
6. N. F. Casey, J.L. Taylor, “The evaluation of wire ropes by acoustic emission techniques”, British Journal of Non-destructive Testing Nov (1985)351-356.
7. K. M. Holford, “The non-destructive testing of wire rope by acoustic emission”, Ph.D. thesis, University College, Cardiff, (1987)
8. G. Rebel, R. Verreet, I.M.L. Ridge, “Lightweight ropes for lifting applications”, OIPEEC Conference , Athens, March 2006, pp. 33-54
9. http://www.pacndt.com/
10. M. Tomic, J. Elazar, Z. Djinovic, “Low-coherence interferometric method for measurement of displacement based on a 3x3 fibre-optic directional coupler”, J. Opt. A: Pure Appl. Opt. 4(2002) 381
11. Z. Djinovic, M. Tomic, A. Vujanic, “Nanometer scale measurement of wear rate and vibrationsby fiber-optic white light interferometry”, Sensors and Actuators A, A123-124 (2005) 92
12. M. Tomic, Z. Djinovic, “Strain and Deformation Measurement Using Intrinsic Fiber Optic Low Coherence Interferometric Sensor”, Proceedings of the 32nd international convention on information and communication technology, electronics and microelectronics, MIPRO 09, Opatija, Croatia, 25.-29. May 2009
13. N. F. Casey, H. White, J. L. Taylor, J. L. “Frequency analysis of the signals generated by the failure of constituent wires of wire rope”, Non-destructive Testing International 18 (1985) 339
14. C. K. Kirkendall, A.Dandridge, “Overview of high performance fibre-opticSensing”, J. Phys. D: Appl. Phys. 37 (2004) R197